Heliyon 5 (2019) e02790

Contents lists available at ScienceDirect

Heliyon

journal homepage: www.heliyon.com

Heliyon

Research article

Light transmission and internal scattering in pulsed laser-etched partially-transparent silicon wafers

Muhd Hatim Rohaizar, Suhaila Sepeai *, Nurfarizza Surhada, N.A. Ludin, M.A. Ibrahim, K. Sopian, Saleem H. Zaidi

Solar Energy Research Institute (SERI), Universiti Kebangsaan Malaysia, 43600, UKM Bangi, Selangor, Malaysia

ARTICLE INFO

Keywords:
Energy
Nanotechnology
Optics
Materials characterization
Materials physics
Trench
Thru-holes
Thermal image
IR transmission
Partial transparent
Silicon wafer

ABSTRACT

Continuing trend in silicon wafer thickness directed at cost reduction approaches basic boundaries created by: (a) mismatch between Al paste and Si wafer thermal expansion and (b) incomplete optical absorption. With its symmetrical front and back electrical contacts, the bifacial solar cell setup reduces stress due to mismatch thermal expansion, decreases metal use and increases high temperature efficiency. Efficiency improvement is accomplished in bifacial solar cells by capturing light from the back surface. Partially transparent wafers provide an option to improve near-infrared radiation absorption within Si wafer. To fully absorb optical radiation, three-dimensional texture of these kinds of wafers is essential. Pulsed laser interactions, thermal oxidation, and wet chemical etching are included in this research. A feature of its energy and pattern setup is the interaction of pulsed laser with Si, running at 1.064 μm wavelength and micro-second length. Two experimental settings were explored: (a) post-laser chemical etching with potassium hydro-oxide etching with thermal oxide as etching mask and (b) post-laser heat Si surface oxidation. Due to fast melting and recrystallization, laser pulsed processing inherently produces its own texture. Some of these spherically-shaped, randomly focused characteristics improve inner scattering and boost near-infrared absorption within the wafer. These characteristics are separated during chemical etching with the thermally-grown oxide layer as an etch mask. Comparison of optical absorption in both surfaces shows almost a rise in the magnitude of absorption in non-etched surfaces. Detailed optical (optical microscope and IR absorption), morphological (field emission scanning electron microscope) and heat imaging (far IR camera) analyses were performed to comprehend physical processes that contribute to near-IR absorption improvement. Such kinds of partially-transparent, three-dimensional textured Si wafers are anticipated to discover applications for bifacial solar cells as substrates.

1. Introduction

Bifacial solar cell refers to a specially-designed configuration in which light is absorbed from both front and rear surfaces [1]. Bifacial solar cells are desirable due to their specific features including superior temperature coefficient, reduced metal usage, ability to fabricate on thinner wafers, and enhanced power output at lower material costs [2, 3]. Bifacial solar cell configuration works well in a vertical configuration [3] and can be applied as structural components such as fence or wall in building integrated photovoltaic systems. Additional sunlight can be coupled into the rear surface to significantly increase its output through placement of a suitable reflector on the backside of a bifacial solar module.

In conventional application of bifacial solar panel, the transparent space between adjacent bifacial cells allows sunlight transmission. The transmitted light is incident on appropriately designed reflectors to direct light back to the rear surface of the bifacial cell. This method is potentially enhancing the output of the bifacial solar panel, albeit at the cost of larger panel size. Therefore, this limitation can be eliminated through specially designed partially transparent bifacial solar cell panel as described in Fig. 1. In this configuration, there is minimal space between the solar cells, instead, the wafer itself becomes partially transparent (Patent: WO 2015/187002 A1). A diffuse reflector placed behind the panel directs this light back to the rear surface. Therefore, in this configuration, the panel size stays the same as any conventional monofacial solar cell panel while its output is enhanced.

In this study, three-dimensional (3D) texturing of partially transparent wafers has been investigated by pulsed laser interactions. The 3D texturing in partially transparent Si wafers is one of the elegant solution

* Corresponding author.
E-mail address: suhailas@ukm.edu.my (S. Sepeai).

https://doi.org/10.1016/j.heliyon.2019.e02790
Received 27 November 2018; Received in revised form 4 July 2019; Accepted 31 October 2019

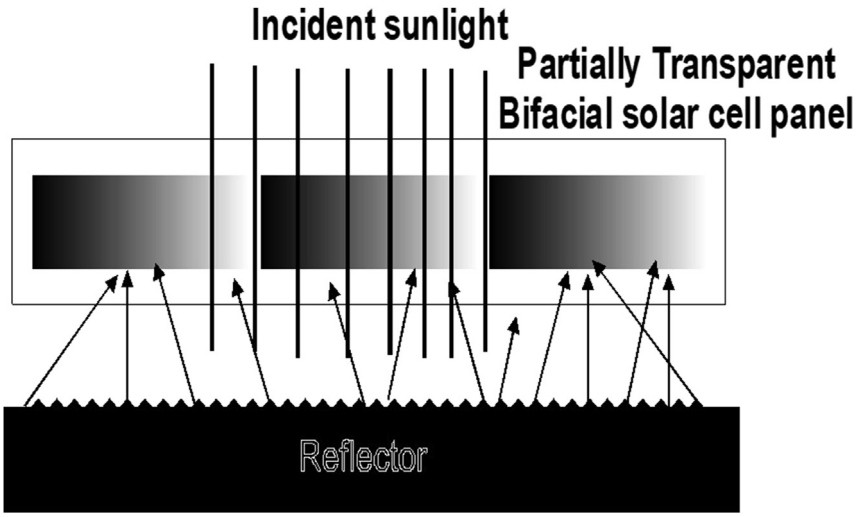

Fig. 1. Partially transparent bifacial solar cell with backside external reflector to direct light to the rear surface of the solar cell.

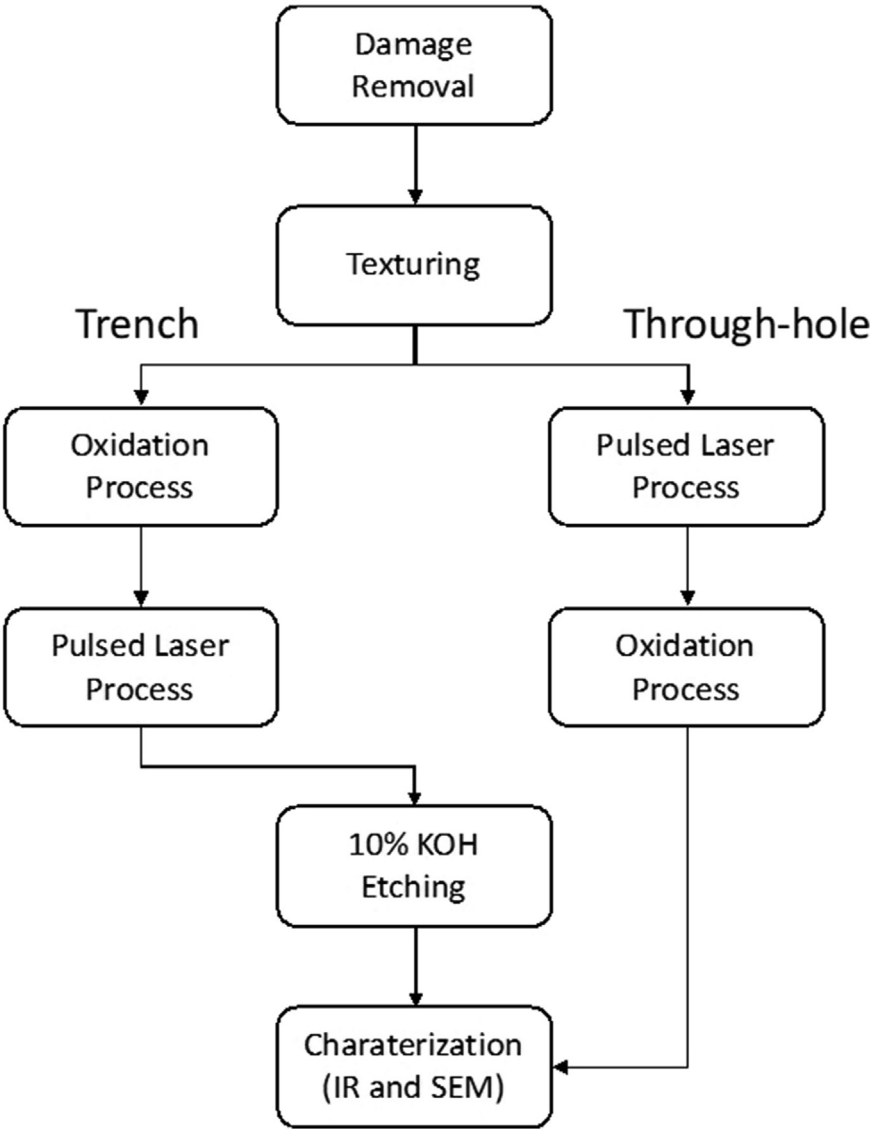

Fig. 2. Trench and through hole formation with texturing processes.

to enhance optical absorption in bifacial solar cells. Pulsed laser processing has been chosen due to less heterogeneous illumination and less steep temperature gradient. Pulsed laser processing has the ability to reduce surface reflectance following random texturing introduced through melting, ablation, and recrystallization [4]. Therefore, in this paper, the development and analysis of pulsed laser etched of partially transparent Si wafers will be presented. The analysis of partially transparent Si wafers includes the topography and cross-section images by Field Emission Scanning Electron Microscope (FESEM), the infra-red (IR) transmission and infrared radiation. Those analyses mentioned provide characterization data that will determine the ability of partial transparent wafer in allow light to transmit to rear region based on hole array developed by pulsed laser interaction. Development of hole array on textured surface build upon Lambertian scattering scheme provide light propagation that can be applied in bifacial solar cell in increasing the capacity of power generated.

2. Methodology

Fig. 2 describes process flow diagram for fabrication of 3D-textured, partially transparent Si wafers. Starting wafers were p-type <100> mono-crystalline Si with a sheet resistivity in a range of 0.5–3 Ω cm at a thickness of approximately 200 μm. As-received wafers were subjected to saw damage removal etch process in 10 % Sodium Hydroxide (NaOH) solution for 15 min at a temperature of 70 °C. Subsequently, planar wafers were textured in KOH, IPA, and deionized water in 1:5:125 volume ratio for 30 min at 70 °C. The thickness measure on textured Si wafer was 165–170μm. Following texture process, two different pulsed laser based texturing processes were investigated. The process performed on textured Si due to avoid wafer etch to very thin wafer during wet-chemical etching process. In additional, textured wafer able to reduce scratching on non-laser rear surface during pulsed laser process. If pulsed laser performs on planar Si, laser array and non-laser area vigorously etch during wet-chemical process and thickness may achieve 100–110μm.

In this study, two process were conducted with different prioritize on oxidation process and pulsed laser processing to determine suitable process in forming partial transparent Si wafer in order to fabricate partial transparent bifacial solar cell. In process 1, also referred to as the Trench Process, thermal oxidation process was carried out prior to pulsed-laser etching. While in process II, also referred to as the thru-hole Process, pulsed-laser processing was done on non-oxidized wafers. An oxide film was grown after pulsed laser process; no wet-chemical etching was done in process II. The thermal oxide layer was grown in an oxidation furnace at 1000 °C for 1 h in oxygen ambient.

The pulsed laser etching was carried out at 23.5 W and 39.6 W under 15 kHz pulse frequency. The equipment used for pulsed etching was part of a semiconductor laser dicing system (YMS-50D). The laser emits at near-infrared invisible light beam with 1.064μm wavelength and beam size at 0.5mm. The pulsed laser wavelength at 1.064 mm was chosen due to weak absorption and long penetration depth to facilitate formation of vertically-etched through holes [5]. With its long micro-second pulse duration, laser interaction allows thermal like molten deposition and heat affected zone (HAZ) at the edge [6]. Some of these debris can be removed by the short-etching process. Two laser power setting were used to create different depth and pathway of hole array for light to transmit to rear surface. Post laser chemical etching was carried out in 10 % KOH solution at a temperature of 70 °C for etching times up to 40 min. The etching time defined the thickness and pattern of the wafers.

Fig. 3 illustrates the pulsed laser-based etch patterns in the Si wafer. The pattern design process was based on CNC motion control software that controls MPC02 two-axis translation stage. Fig. 3(a) describes the through hole pattern with 0.5 mm diameter. Fig. 3(b) describes the design used to form a ring shape pattern with 0.5 mm diameter and trench gap between 18-50μm. The distance between holes was 2 mm for both patterns. Table-1 summarizes process details on all the samples investigated in this study. Samples A and B were from Trench pattern while samples C and D were from Through-hole pattern. Samples A and C were etched at laser power of 23.5 W and samples B and D etched at laser power of 39.6 W.

Three main characterization processes were investigated. For 3D texture evaluation, Hitachi Field Emission Scanning Electron Microscopy (FESEM) system was employed. SEM images provide necessary information in order to determine texture dimensions and wafer thickness. Fig. 4 shows a schematic diagram for Infra-red (IR) Transmission of partial transparent wafer that was characterized with a variation of etching time. The system is designed to measure optical IR transmission for wavelengths between 0.8 μm to 1.5 μm. The observation on microscopic surface structure of the wafer after through each process and optical transmission measurements help determine influence of surface texture on absorption. The infrared radiation was measured under the sun intensity at AM1.5 or 1 kW/m^2 using Fluke Ti-32. This testing was performed in order to evaluate heat accumulation and temperature different on each of samples.

3. Results and discussion

3.1. Field emission scanning electron microscope analysis

Scanning electron microscope measurements were used to analyse features of seven samples described in Table-1. Fig. 5 shows SEM pictures

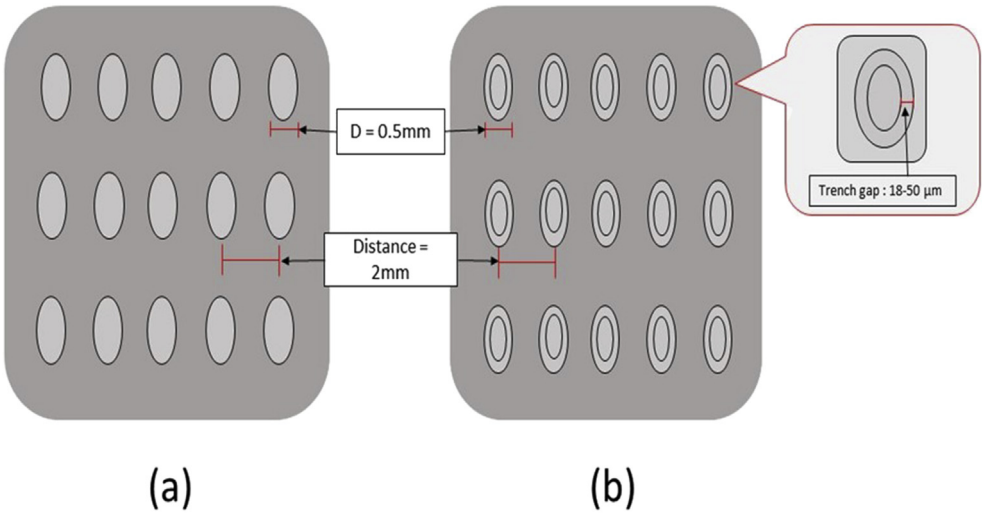

Fig. 3. (a)Through hole and (b)donut shaped trench patterns formed with pulsed laser system YMS-50D.

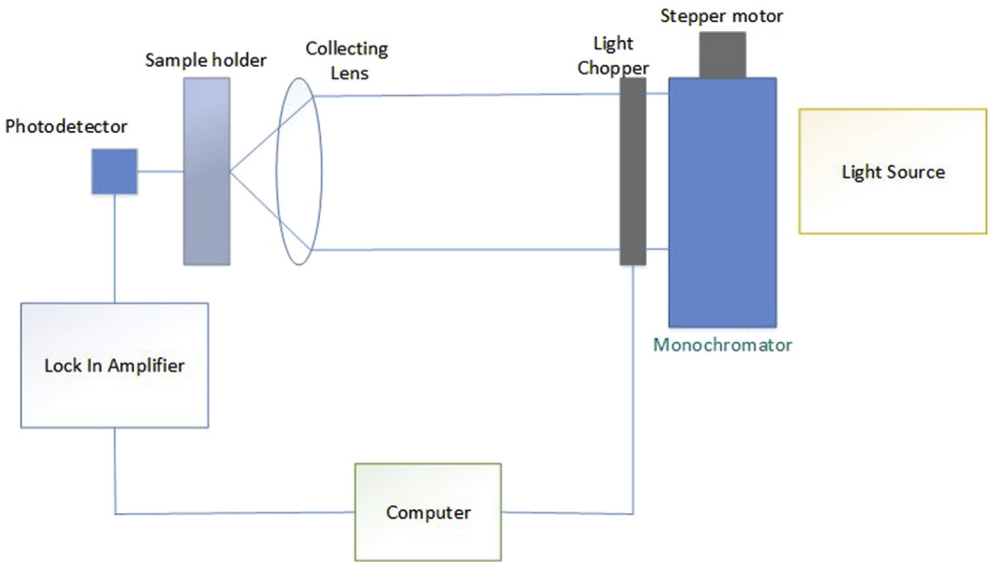

Fig. 4. Schematic diagram for IR transmission measurement system.

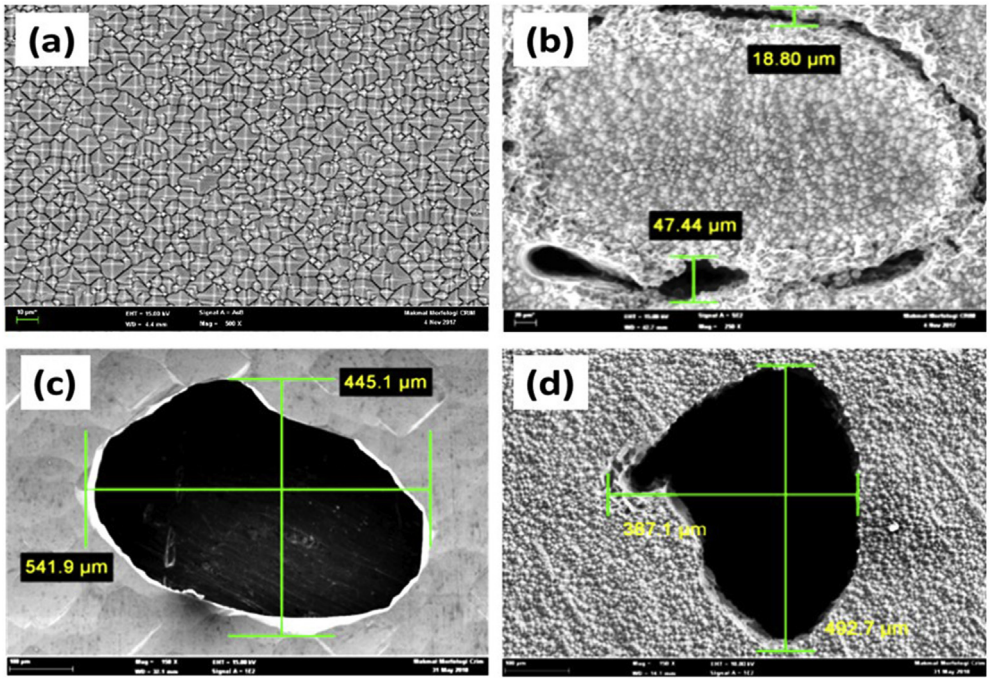

Fig. 5. Top view SEM pictures of silicon wafer with (a)textured, (b)trench, (c)through holes on planar and (d)through holes on textured.

of four kinds of textured and etched samples investigated in this study. Fig. 5(a) illustrates top view of the Random pyramids textured wafer prior to pulsed. Fig. 5(b) shows top view of the pulsed laser etched donut pattern with trench width of approximately 20 μm Fig. 5(c) shows top view SEM picture of through hole with a diameter of approximately 500 μm Fig. 5(d) shows the same pattern etched on a textured surface; pattern periodicity follows the dimensions described in Fig. 3. Fig. 6 shows cross-sectional SEM views of both trench (Fig. 6(a)) and thru-hole patterns. The surface roughness is higher on trench sidewalls in comparison with through holes; wafer thicknesses are comparable (see Figs. 7 and 8).

The sizes of the randomly-textured pyramids were 3-9-μm range with heights in 3–10 μm range. The variation in laser power produced same patterns but at varying heights with depth increasing with energy. Therefore, pulsed laser and KOH etching processes were controlled in order to form partially and completely etched patterns through the Si wafer. The role of KOH etching was to remove residue from laser etching resulting in relatively smooth surfaces.

Based on SEM analysis, surfaces with pyramidal texture on front and rear surfaces have been uniformly created. Pulsed laser processing has trench and thru-hole configurations. KOH etching and thermal oxidation were used to remove and preserve laser-induced surface and sidewall texture respectively. Surface texture on front, rear, and sidewalls contributes to enhance internal three-dimensional texturing. Surface reflection is also reduced by surface texturing based on diffractive and physical optics [7]. Reduction in reflection losses leads to higher transmission. Lambertian scattering plays a major role; its application to a bifacial solar cell is illustrated in Fig. 7. Fig. 7 is used as exact analytical solution to described light propagation and simplify analytical formula that applies for weakly and strongly absorbed light. According to *Richter et.al* [8], the upper limit for 1-sun energy conversion efficiency of crystalline Si solar

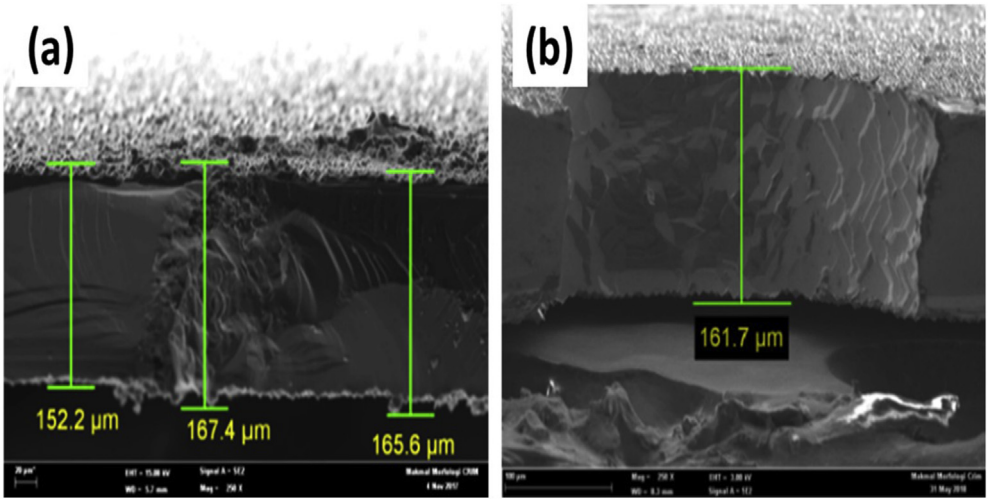

Fig. 6. Cross-sectional SEM pictures of patterns for (a)trench and (b)thru-hole.

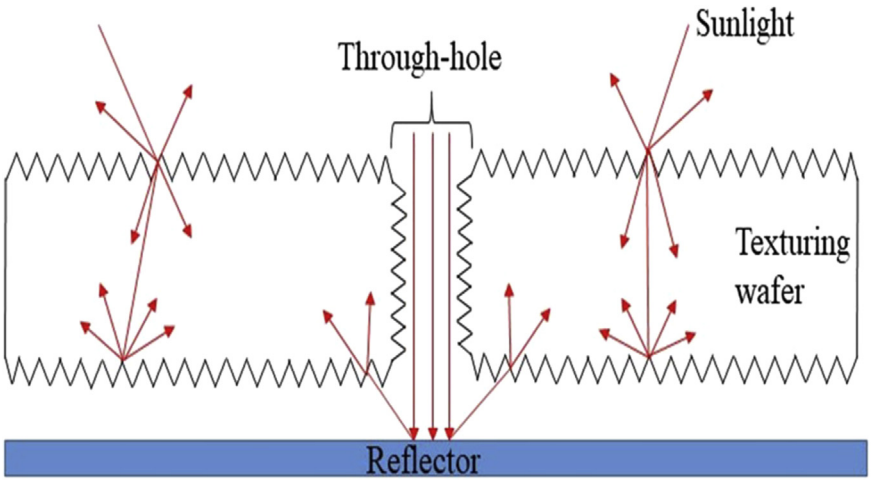

Fig. 7. Lambertian texturing in 3D-teturing of silicon wafers.

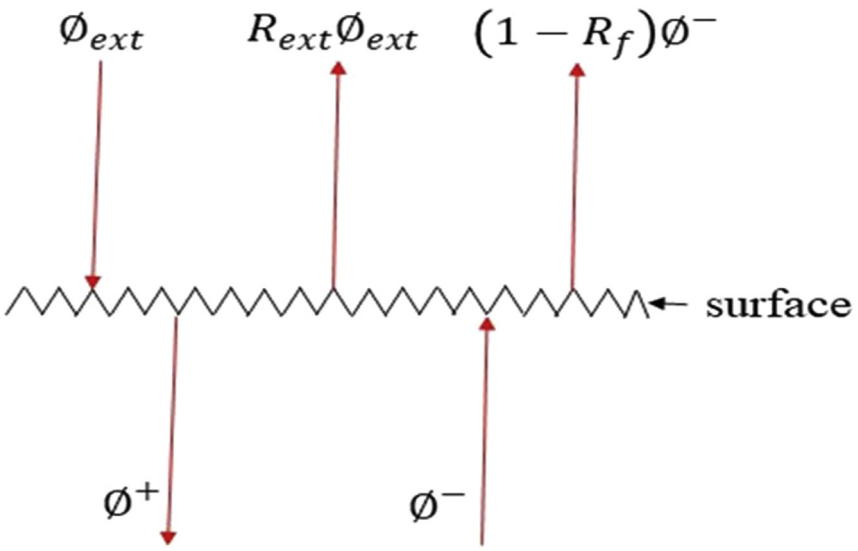

Fig. 8. Relationship between internal and external downward and upward hemispherical fluxes (Adapted from [10]).

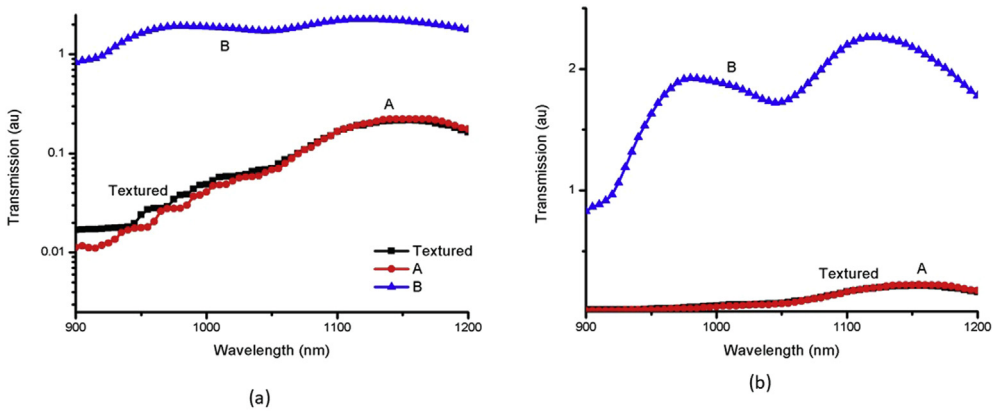

Fig. 9. (a). Optical transmission measurements as a function of wavelength textured and trench samples at different laser power of A = 23.5W, B = 39.6W (semi log-scale).(b). Optical transmission measurements as a function of wavelength textured and trench samples at different laser power of A = 23.5W, B = 39.6W (linear scale).

cell with Lambertian light trapping has been calculated to be 29.43 % for a non-doped cell of optimum thickness of 110 μm at 298.15 K. Lambertian surface capable of filling all the available k-space with light beams of equal intensity is difficult to achieve in practice [9]. Three-dimensional, pulsed laser etched surfaces are attractive candidates due to their light trapping along all three directions.

As described in Fig. 8, light propagation through textured wafer is described as a downward hemispherical flux (ϕ^+) and an upward flux (ϕ^-). The surface area is possible to equate the difference between downward and upward fluxes for internal and external of the device;

$$\varnothing_{ext} - \left[R_{ext}\varnothing_{ext} + \left(1 - R_f\right)\varnothing^- = \varnothing^+ - \varnothing^-\right. \tag{1}$$

Where R_{ext} is appropriately weighted initial area reflection of reflection of the external flux $\varnothing_{ext}$ and R_f is internal upward flux from the front surface [10].

According to Green [10], incident light on a textured solar cell surface is randomized inside the substrate and attenuates as it propagates inside by varying amount depending on its direction of propagation. Light incident on the rear surface is once again re-randomized with the same fraction of the reflected light reaching the top surface as the fraction reaching the back, therefore,

$$T_a^+ = T_a^- = T_a(\alpha W) \tag{2}$$

Where T_a is single-pass transmission for this case:

$$T_a(\alpha W) = \frac{\int_0^{2\pi}\int_0^{\frac{\pi}{2}} \exp\left(-\frac{\alpha W}{cos\theta}\right) cos\theta sin\theta d\theta d\varnothing}{\int_0^{2\pi}\int_0^{\frac{\pi}{2}} cos\theta sin\theta d\theta d\varnothing} = 2\int \exp\left(-\frac{\alpha W}{cos\theta}\right) cos\theta d(cos\theta) \tag{3}$$

3.2. IR transmission

For solar cells, optimum texture is generally recognized to be in the form of randomly textured pyramids (Fig. 5(a)). Therefore, in all IR transmission measurements reported here, transmission response with textured wafer has been included as a bench mark. All IR transmission measurements have been plotted in log scale since there are several orders magnitude variations in the transmitted signal. As described in Table-1, samples A and B represent trench patterns with increasing laser energy and longer depths. The samples C and D belong to the thru-hole pattern family with increasing energy. The thru-hole in sample C does not etch all the way to through the wafer, while sample D represents a true thru-hole.

Fig. 9a and b plots of semi log and linear scale for the transmission response in 900–1200 nm spectral range of textured (no laser) and trench samples at increasing laser power, incident laser power were 23.5 W and 39.6W on samples A and B respectively. It is noted that the trench with high power laser (sample B) has substantially higher transmission in comparison with low laser power (sample A). Sample A also exhibits lower transmission than the textured at shorter (~ 900–1000 nm) and matches with it at longer wavelengths. Pulsed laser process creates surface and sidewall roughness that is likely responsible for enhanced absorption and lower transmission of the trench pattern. Light penetration measurements recorded in terms of pictures of the transmitted light at the rear surface using a Canon lens EFS 19–55mm camera under ISO 3200 (Fig. 10) shows sample A was unable while sample B was able to transmit light to rear surface.

Fig. 11a and b plots of semi-log and linear scale to shows comparison of IR transmission measurements of thru-hole samples on planar at increasing laser powers where sample C etched at 23.5 W does not support true thru-hole while samples D & E etched at 39.6 W represent true thru-hole. The difference between D & E lies in surface texture with D planar and E textured as described in Table 1. It is noticed that the randomly textured wafer shows the lowest transmission. Sample D (high laser power on planar) shows the highest transmission followed by E and sample C (low laser power on planar). An interesting effect is observed in sample C which exhibits absorption smaller or comparable to textured wafer. This is attributed to enhanced absorption in laser-crystallized random surfaces which were subjected to thermal oxidation and not removed by KOH etching. Therefore, at lower laser power, laser creates its own texture due to rapid melting and recrystallization, which significantly enhance internal scattering resulting in higher absorption even though significant fraction of Si was etched off by laser process.

Samples D and E shows identical pattern at different transmission levels. It is also noted that despite identical pattern configuration, textured wafer (sample E) transmission is significantly lower than that of the planar surface. This is attributed to internal scattering from the randomly-textured pyramids and is captured in the rear surface light transmission pictures captured by Canon lens EFS 19–55mm camera under ISO 3200 (Fig. 12). Sample E exhibits significantly higher brightness and uniform penetration in comparison with sample D due to diffractive and geometrical scattering from randomly-distributed pyramidal textured surfaces on the front and rear surfaces.

In order to evaluate relative transmission, Fig. 13a (semi-log scale) and 13b (linear scale) show IR transmission measurements of all five samples described in Figs. 9 and 11. It is noticed that samples with thru holes have higher transmission compared to the trench samples and transmission increases with laser power. Table 2 shows the different of light transmission at 1000 nm wavelength for all samples.

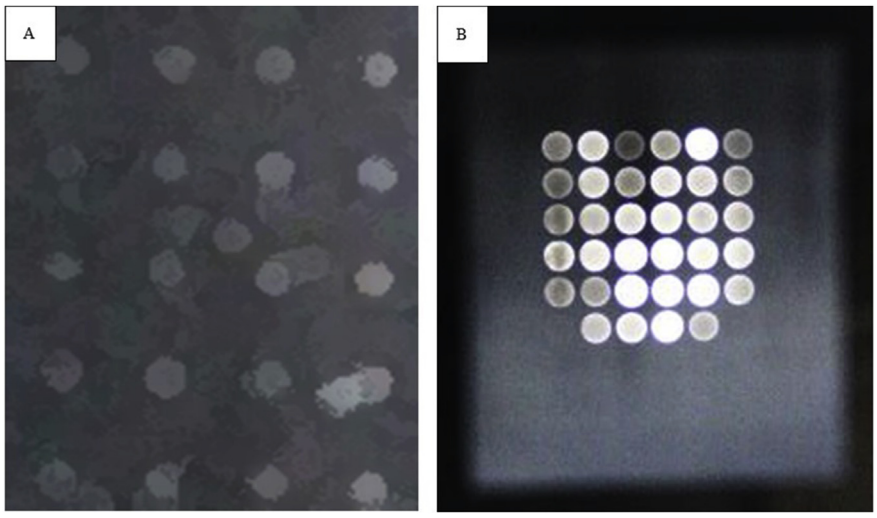

Fig. 10. Back side pictures of transmitted light from trench samples at different laser power where A = 23.5 W and B = 39.6 W.

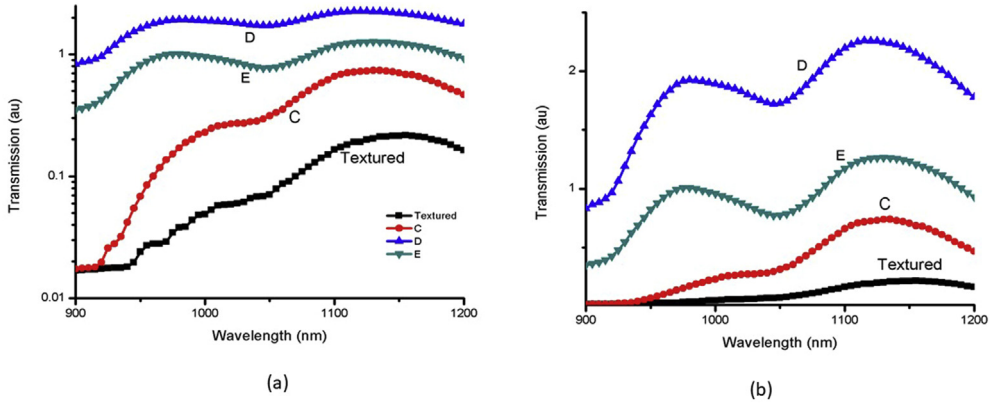

Fig. 11. (a). Optical IR transmission measurements as a function of wavelength in semi log-scale graph (Textured, C = planar with 23.5W laser induction, D = planar with 39.6W laser induction, E = textured with 39.6W).(b). Optical IR transmission measurements as a function of wavelength in linear scale graph (Textured, C = planar with 23.5W laser induction, D = planar with 39.6W laser induction, E = through hole textured with 39.6W).

Table 1
Description of samples investigated in this study.

No.	Name	Pulsed Laser Pattern	Pulsed Laser Power (Watt)	Process Description	Comments
1	Planar	None	NA	Saw damage removal	Baseline reference
2	Textured	None	NA	Saw damage removal and texturing	Pyramidal texture reference
3	A	Trench	23.5	KOH etching with oxide mask	Laser-induced texture removed
4	B	Trench	39.6	KOH etching with oxide mask	Laser-induced texture removed
5	C	Through hole (planar)	23.5	Oxide growth	Laser texture oxidized
6	D	Through hole (planar)	39.6	Oxide growth	Laser texture oxidized
7	E	Through hole (textured)	39.6	Oxide growth	Laser texture oxidized

From the IR transmission measurement analysis, it is clear that more light passes through the thru-hole pattern in comparison with the donut-shaped trench. This is agreement with transmission definition in optics that in traversing through a weakly absorbing medium, electromagnetic waves (either visible light, radio waves, ultraviolet or IR) transmission can be substantially reduced scattering off the surfaces. In this study, it was observed that the donut-shaped trench absorption was substantially higher than thru-hole. This is because of the internal scattering in trench was higher due to the double texture pattern. The double texture in trench were pyramid texture from KOH etching and texture produced by the laser due to the rapid melting process. The increase of internal scattering in donut-shaped trench significantly increases the near IR absorption in the Si wafer. Therefore, their transmissions were lower than thru-hole samples. Despite of the lower transmission of the trench pattern, it is not fair yet to conclude that this pattern is not suitable for the application on partial transparent bifacial solar cell. This donut-shape trench pattern may be produce better output efficiency for the rear surface in partial transparent bifacial solar cell due to the more light were absorbed and higher photogeneration produced.

Meanwhile, the thru-hole pattern (C, D and E) show higher transmission compared to donut-shaped trench pattern. In thru-hole configuration, light passed through the wafer without scattering. The thru-hole pattern produced a successful partial transparent Si wafer. This can be determined by the IR transmission output and the pictures of transmitted

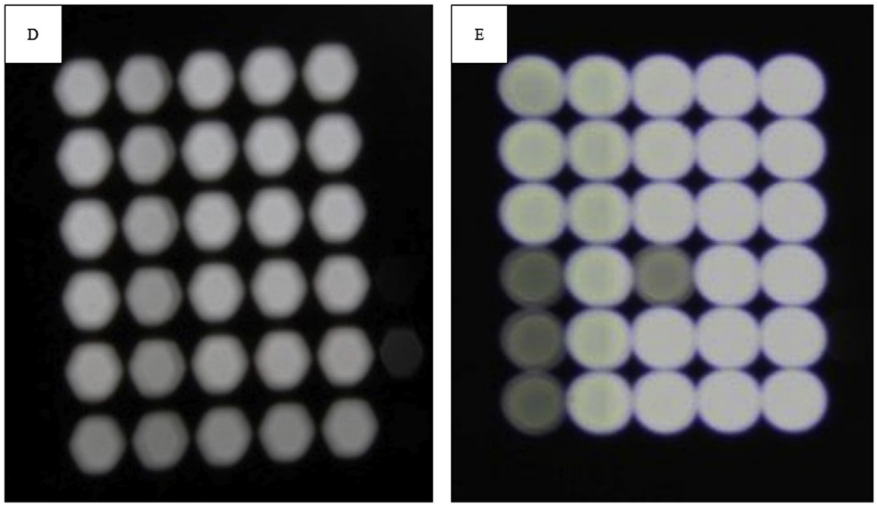

Fig. 12. Pictures if transmitted light from planar (D) and textured (E) through hole surfaces.

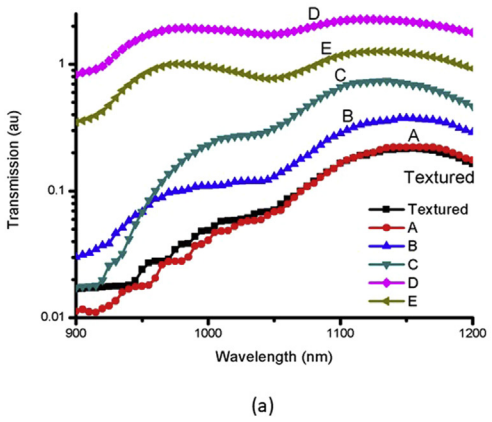

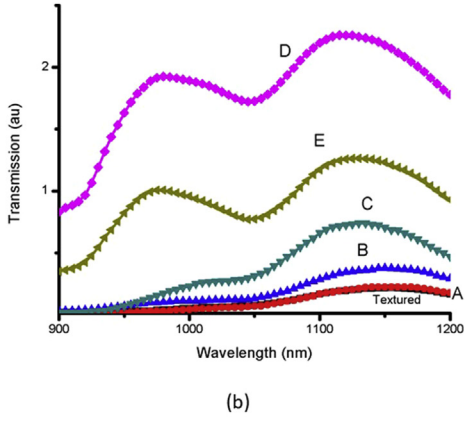

Fig. 13. (a). Comparison of optical IR transmission measurements as a function of wavelength in semi log-scale graph (Textured, A = trench with 23.5W laser induction, B = trench with 39.6W laser induction, C = planar with 23.5W laser induction, D = planar with 39.6W laser induction, E = through hole textured with 39.6W).(b). Comparison of optical IR transmission measurements as a function of wavelength in linear scale graph (Textured, A = trench with 23.5W laser induction, B = trench with 39.6W laser induction, C = planar with 23.5W laser induction, D = planar with 39.6W laser induction, E = through hole textured with 39.6W).

Table 2
Different of light transmission at 1000 nm wavelength.

Sample	Transmission (au)
Textured	0.04861
A	0.04091
B	0.10943
C	0.22888
D	1.89266
E	0.95731

light from the rear side for sample D and E. The thru-holes samples were the best candidate to be applied as partial transparent bifacial solar cell as it is a 3D texturing that become new approach to enhance optical absorption in bifacial solar cell. This thru-hole wafer with higher transparency will allow sunlight transmission in the bifacial solar cell itself due to the existing of transparent space between adjacent solar cells. Therefore, the aim of having higher output at the same panel size of commercial bifacial panel and potential candidate for thinner wafer can be achieved in this configuration.

It is important to note that all the IR transmission output for trench and thru-hole samples were in a good agreement with Beer-Lambert Law. The Beer-Lambert Law [11] defines transmission (T) as;

$$T = \frac{I}{I_o} \tag{4}$$

where I is the light intensity after it passes through the sample and I_o is the initial light intensity. Therefore, in either trench or through holes, if I is less than I_o, then obviously the sample has absorbed some of the light. The relationship between the absorbance (A) and the two intensities is given by;

$$A = -log_{10}\ T = -log_{10}\ \frac{I}{I_o} \tag{5}$$

The absorbance ranges from 0 to 1. An absorbance of 0 at some wavelength means that no light of that particular wavelength has been absorbed. The intensities of the sample and reference beam are both the same, therefore the ratio of I_o/I is 1. Log_{10} of 1 is zero. An absorbance of 1 happens when 90% of the light at that wavelength has been absorbed - which means that the intensity is 10% of what it would otherwise be. In that case, I_o/I is 100/I0 (=10) and log_{10} of 10 is 1. From Fig. 13 on comparison of all samples, it can be seen that sample D with highest transmission shows the transmission value of higher than 1. This indicates that almost highest partial transparent of Si wafer with thru-hole pattern was obtained. The investigation on the performance of this pattern as partial transparent bifacial solar cell will be investigated in further research.

3.3. Infrared radiation

Infrared radiation emission measurements were carried out in order to evaluate temperature response as a function of surface texture. These far

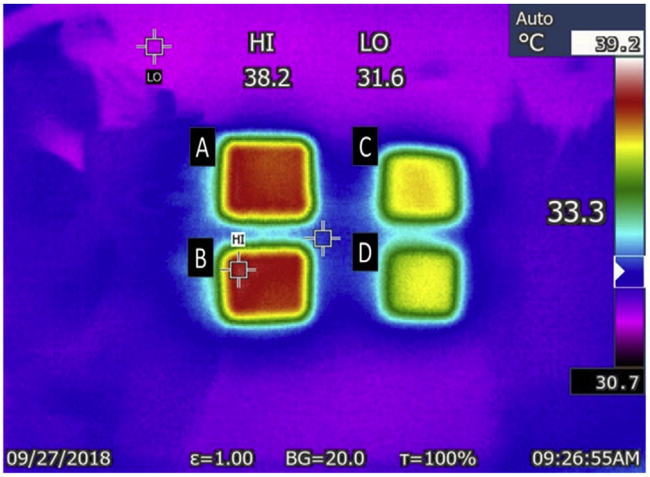

Fig. 14. Thermal images of infrared radiation (A = trench with 23.5W laser induction, B = trench with 39.6W laser induction, C = planar with 23.5W laser induction, D = planar with 39.6W laser induction).

IR measurements were carried out with Ti-32 thermal imager under sunny conditions at 30 °C for 5 min. The emissivity, ε was set at 1 and thermal heat, T at 100 %. Fig. 14 shows four types of samples are tested to observe influence of texture on absorption and temperature. The tested wafers were trench (A and B) and thru-hole (D and E). According to thermal image, the highest temperature of 38.2 °C was measured on samples A & B which indicated that trench samples absorb most radiation and consequently reach higher surface temperatures. In addition, donut-shaped trench also has internal scattering which increases the near IR absorption in the Si wafer. While samples D and E exhibited significantly lower temperature presumably due to high transmission of thru hole samples. This image was in a good agreement with IR Transmission result.

4. Conclusion

The 3D texturing produced for partially transparent wafers were based on trench and thru-hole geometric configurations formed with pulsed laser in combination with chemical etching and thermal oxidation of Si. The analysis was based on surface morphology, IR transmission, optical, and thermal imaging of all samples. The roughness of trench samples was higher than the thru-hole in part due to the extra texture produced from the rapid melting and recrystallization during post-laser process. The thru-hole samples produced higher transmission compared to trench samples. The lower transmission of trench samples was attributed to internal scattering that significantly enhanced the near IR absorption. The clear image of transmitted light from the rear side with planar and textured front surfaces revealed the impact of internal scattering. Thermal image analysis on both trench and thru-holes demonstrated that donut shaped trench pattern absorbed more sunlight. This is manifested in the higher surface temperature of trench samples. Future work on the application of partial transparent bifacial solar cell on both trench and thru-hole samples will be conducted to investigate the performance output.

Declarations

Author contribution statement

Muhd Hatim Rohaizar: Conceived and designed the experiments; Performed the experiments; Analyzed and interpreted the data; Wrote the paper.

Suhaila Sepeai & Saleem H. Zaidi: Conceived and designed the experiments; Analyzed and interpreted the data; Contributed reagents, materials, analysis tools or data; Wrote the paper.

Nurfarizza Surhada: Performed the experiments.

N. A. Ludin, M. A. Ibrahim & K. Sopian: Contributed reagents, materials, analysis tools or data.

Funding statement

This work was supported by Malaysia Ministry of Energy, Science, Technology, Environment and Climate Change (MESTECC) (03-01-02-SF1322). This work was also supported by Malaysia Ministry of Education (FRGS/1/2018/STG02/UKM/02/5).

Competing interest statement

The authors declare no conflict of interest.

Additional information

No additional information is available for this paper.

References

[1] C.K. Lo, Y.S. Lim, S.Y. Kee, Improvement of bifacial solar panel efficiency using passive concentrator and reflector system, in: Proc. 2013 Int. Conf. Renew. Energy Res. Appl. ICRERA 2013, No. October, 2013, pp. 42–45.
[2] S. Sepeai, et al., Design optimisation of bifacial solar cells by PC1D simulation, J. Energy Technol. Policy 3 (5) (2013) 1–11.
[3] B. Soria, E. Gerritsen, P. Lefillastre, J.E. Broquin, A study of the annual performance of bifacial photovoltaic modules in the case of vertical facade integration, Energy Sci. Eng. 4 (1) (2016) 52–68.
[4] M.C. Gupta, D.E. Carlson, Laser processing of materials for renewable energy applications, MRS Energy Sustain. 2 (January 2015) (2015) E2.
[5] S. Subramonian, M.S. Kasim, M.A. Ali, R. Izamshah, R. Abdullah, Micro-drilling of silicon wafer by industrial CO 2 laser, Int. J. Mech. Mater. Eng. (2015) 2–7.
[6] F.A. Lasagni, A.F. Lasagni, Fabrication and characterization in the micro-nano range, Adv. Struct. Mater. 10 (2011) 361–377.
[7] K. Burgi, M. Marciniak, M. Oxley, S. Nauyoks, Measuring the reflection matrix of a rough surface, Appl. Sci. 7 (6) (2017) 568.
[8] A. Richter, M. Hermle, S.W. Glunz, Crystalline silicon solar cells reassessment of the limiting efficiency for crystalline silicon solar cells, IEEE J. Photovolt. 3 (4) (2013) 1184–1191.
[9] K. Inframerah, S.S. Silikon, Infra-red investigation ON silicon solar cells, Malays. J. Anal. Sci. 21 (5) (2017) 1134–1142.
[10] M.A. Green, Lambertian light trapping in textured solar cells and light-emitting diodes: analytical solutions, Prog. Photovolt. Res. Appl. 10 (4) (2002) 235–241.
[11] T.G. Mayerhöfer, J. Popp, The electric field standing wave effect in infrared transflection spectroscopy, Spectrochim. Acta Part A Mol. Biomol. Spectrosc. 191 (2018) 283–289.